

Shot-to-shot and average absolute photon flux measurements of a femtosecond laser high-order harmonic photon source

T Leitner¹, A A Sorokin^{2,3,5}, J Gaudin⁴, H Schoeppe², U Kroth², K Tiedtke³, M Richter² and Ph Wernet¹

¹ Institute for Methods and Instrumentation for Synchrotron Radiation Research, Helmholtz-Zentrum Berlin GmbH, Albert-Einstein-Str. 15, 12489 Berlin, Germany

² Physikalisch-Technische Bundesanstalt, Abbestr. 2-12, 10587 Berlin, Germany

³ Deutsches Elektronen-Synchrotron DESY, Notkestr. 85, 22607 Hamburg, Germany

⁴ European XFEL, Albert-Einstein-Ring 19, 22761 Hamburg, Germany

⁵ Ioffe Physico-Technical Institute, Polytekhnicheskaya 26, 194021 St. Petersburg, Russia

E-mail: leitner@helmholtz-berlin.de

Abstract. The absolute flux of a femtosecond Vacuum-Ultraviolet (VUV) photon source based on high-order harmonic generation of a femtosecond Ti:sapphire laser and monochromatized with a grating monochromator is determined both on a shot-to-shot basis and averaged over seconds by a calibrated gas monitor detector. The average flux is compared to the average flux as determined with a calibrated GaAsP semiconductor photodiode. We find that the photodiode is a reliable and easy-to-use tool to estimate the order of magnitude of the average photon flux but that, due to saturation losses, it underestimates the average flux by up to -15%.

Submitted to: *New J. Phys.*

1. Introduction

High-order harmonic generation (HHG) has emerged as a widely used tool to produce bright femto- and attosecond vacuum-ultraviolet (VUV) and soft x-ray pulses [1, 2, 3, 4]. These pulses can be used to study ultrafast atomic, molecular and magnetism dynamics [5, 6, 7, 8, 9, 10] and are bright enough to perform coherent x-ray diffractive imaging for investigations on the nanoscale [11]. Furthermore, the HHG process itself can provide insight into the electronic structure of the generating molecule [12, 13, 14].

One of the key parameters of every photon source is its photon flux. A determination of the absolute flux and of the shot-to-shot fluctuations of the flux is highly desirable. Correct determination of these parameters becomes especially important when exploring the feasibility of new experiments. For example, the photon flux is a crucial parameter when high-harmonic radiation is used to seed a Free Electron Laser (FEL) [15, 16]. Accurate on-line measurements of the photon flux are required when HHG sources are used to investigate non-linear effects in the VUV to spectral range, e.g. for the determination of atomic two-photon ionization cross sections [17, 18]. In general the absolute flux and the shot-to-shot fluctuations are key parameters when optimizing an existing or setting up a new HHG source.

To our knowledge accurate shot-to-shot measurements of absolute fluxes from HHG sources have not been done yet. Nisoli et al. measured shot-to-shot HHG spectra, but did not determine shot-to-shot fluxes [19]. Determination of absolute average fluxes of a HHG source was done in [20] based on a rather complicated scintillator - photomultiplier setup. In [21] a calibrated EUV spectrometer was used to determine absolute photon fluxes but with a standard uncertainty as big as 50%.

Another widespread, easy-to-use tool for measuring photon fluxes are semiconductor photodiodes. In [15, 22, 23], for example, they are used to determine absolute average photon fluxes of HHG sources. Such photodiodes are usually calibrated at quasi continuous-wave (cw) light sources with long pulses in the picosecond regime at high repetition rates (e.g. synchrotrons). The Physikalisch-Technische Bundesanstalt (PTB, Germany's national metrology institute) uses the Metrology Light Source (MLS) for the calibration of photodiodes in the UV-VUV regime [24]. At the Normal-incidence monochromator beamline for UV and VUV detector calibration, pulses of 20 ps pulse duration (FWHM) are delivered with a repetition rate of 500 MHz and peak fluxes of 5×10^{11} photons/s (i.e. 10 photons/pulse). In contrast to that, our HHG setup delivers monochromatized 120 fs FWHM pulses at a repetition rate of 3 kHz with peak fluxes of the order of 10^{19} photons/s (i.e. 10^6 photons/pulse). The average radiant power and the spot size on the diode are comparable for these two sources, hence is the average photon flux density. Thus, if the HHG photon flux is measured with a photodiode, the peak flux or the peak radiant power, respectively, seen by this diode are more than seven orders of magnitude higher than during calibration.

This raises the question, whether the calibration is still correct or if saturation losses significantly contribute to the diode's response in the regime of parameters used here. The rapid generation of a large number of charge carriers in the active area of the diode from femtosecond pulses will not necessarily result in the same response, as will illuminating the diode with a (quasi) cw light source of comparable average power. Enhanced recombination may occur leading to increased saturation loss, meaning that less generated charge carriers reach the

read-out electronics and contribute to the diode's response signal. This effect should intensify with increasing charge carrier density generated by increasing peak powers of the radiation. Therefore saturation loss and erroneous response of the photodiode will rise as well [25, 26, 27].

In order to test whether semiconductor photodiodes are reliable for measuring absolute photon fluxes of high peak power femtosecond sources, we compared the values for the average photon flux of the monochromatized radiation available for experiments from our source measured with a calibrated GaAsP semiconductor photodiode (Hamamatsu model g112704) with those obtained from measurements with a calibrated and validated gas monitor detector (GMD). The GMD is based on the photoionization of a (rare) gas and was developed by PTB/DESY/Ioffe Institute for the on-line measurement of the radiant power of VUV and soft X-ray FELs [28, 29, 30, 31]. Measurements of absolute average photon fluxes as well as shot-to-shot fluctuations with an accuracy of 5% are feasible with this device.

2. Experimental Setup

Our experimental setup is shown in Figure 1, see also [32, 33]. The VUV radiation is produced by a 50 fs, 1 mJ Ti:Sa laser (central wavelength 785 nm) which is focused into a 5.5 mm long gas cell by a $f=500$ mm lens resulting in a focal spotsize of $60 \mu\text{m}$ and a peak intensity of approximately $2 \times 10^{14} \text{W}/\text{cm}^2$. The entrance and the exit of the cell along the laser path are sealed with a thin copper foil (0.1 mm) in which the laser itself drills optimum sized holes for propagating through. In this experiment we used either *Xe* or *Ar* as non-linear medium for generation. We operated the cell at a pressure in the gas inlet tube of 0.46 mbar for *Xe* and 3.2 mbar for *Ar* and a backing pressure outside the cell of 8×10^{-3} mbar or 1.1×10^{-2} mbar, respectively. Thereafter the infrared light is blocked by two aluminum foils (150 nm thick) one before and one after a toroidal grating monochromator to ensure that no fundamental IR photons reach the GMD or the photodiode and influence the measurements, although both detectors are not sensitive to the infrared radiation. The monochromatized VUV pulses then first pass the GMD before they hit the photodiode. The pulse duration, available for experiments after the monochromator is ~ 120 fs FWHM in our setup. This was determined by VUV-IR cross correlation with photoionization sidebands of *Ar* as demonstrated in [34]. The cross correlation measurement was done in a separate experiment to ensure, that no other gas from the photoionization chamber perturbs the GMD signal. The bandwidth of the monochromatized pulses amounts to ~ 140 meV as shown in earlier work [32].

We did the experiment with four different harmonics of the infrared laser (H11, H13, H15, H17) at corresponding photon energies of 17.4 eV, 20.5 eV, 23.7 eV and 26.9 eV. The GMD is based on atomic photoionization of a rare gas at low particle density in the range of 10^{11} to $10^{12}/\text{cm}^{-3}$. Therefore it is indestructible

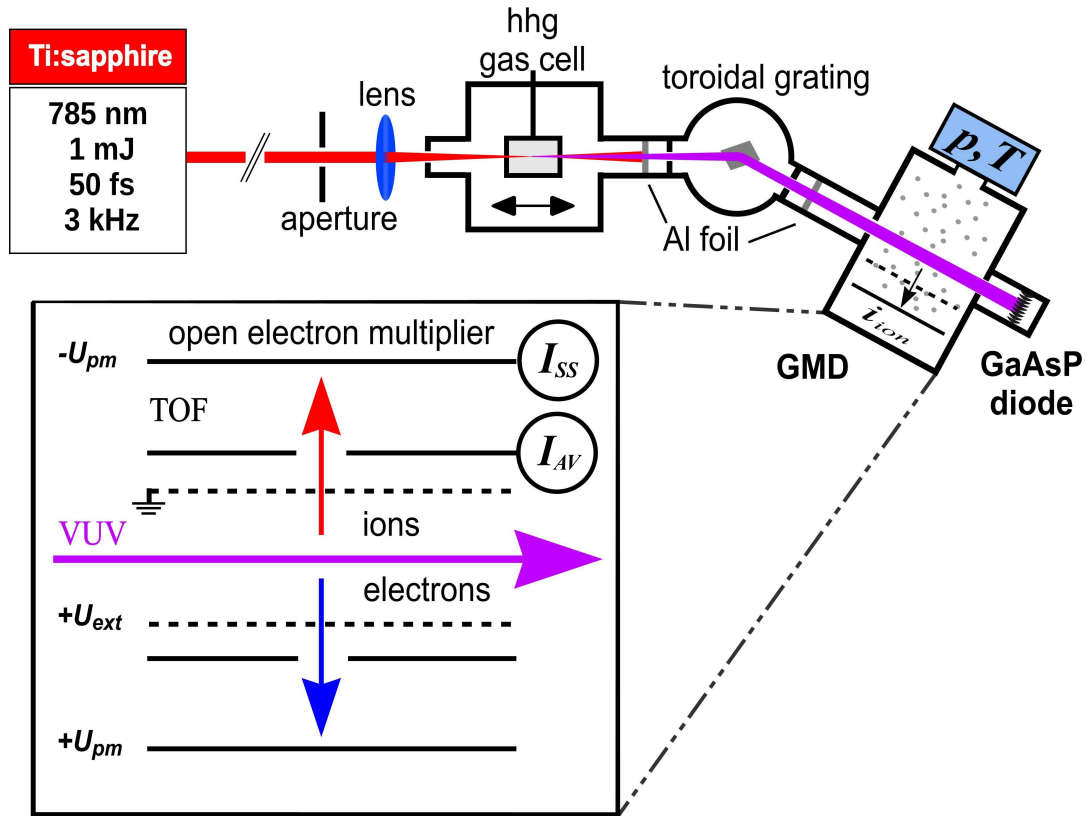


Figure 1. Experimental setup — A 50 fs Ti:Sa laser drives the HHG VUV source, after a toroidal grating the photon flux in the monochromatized VUV beam is measured by the GMD and a standard Hamamatsu GaAsP photodiode. Inset: (principal) sketch of the assembly inside the GMD illustrating its basic functional principle, I_{SS} and I_{AV} denote the single-shot and average signals available from the detector.

and transmits more than 99.5% of the radiation for the photon energy range used in this experiment [35]. The inset of Figure 1 illustrates the functional principle of this detector. The VUV radiation ionizes the target gas (either Xe or Ar in the present work). The generated ions and electrons are extracted and accelerated in opposite directions by a homogeneous static electric field. The extraction field of 333 V/cm (corresponding to an extraction voltage of 1000 V) is chosen to be high enough to ensure complete collection of the charged particles created in the interaction volume accepted by the respective particle detector. In the present experiment the ion signal was measured only. A first simple metal plate detection electrode allows for measuring a slow averaging current I_{AV} by a calibrated Keithley 617 electrometer with a time constant of a few seconds, which is not affected by any individual intra-pulse time structure or shot-to-shot variations of the radiation. Moreover, a fraction of the ions enters a drift section through a small aperture in the detection electrode and is detected by an open electron multiplier (ETP 14880) operated in a linear regime. The multiplier can be used for ion time-of-flight (TOF) spectrum measurements which enables

checking the purity of the target gas as well as possible influences of multi-photon ionization on our measurements as will be discussed later. Furthermore, it can be utilized for pulse resolved (shot-to-shot) relative flux measurements. The signal from the multiplier is read out with the help of a LeCroy digital oscilloscope.

From the measured ion-current signal I_{ion} the average number of photons N_{ph} can be calculated as:

$$N_{ph} = k_{cal} \times \frac{I_{ion}}{n_a(p, T) \times \sigma_{pi}(h\nu)} \quad , \quad (1)$$

where σ_{pi} is the photoionization cross section of the target gas at the used photon energy $h\nu$, k_{cal} is a known detector calibration constant including the length along the photon beam accepted by the detection electrode and the ion detection efficiency. n_a is the target gas density at the given pressure and temperature, determined by $n_a = p/k_B T$ (k_B : Boltzmann constant). As knowing the exact pressure p and temperature T of the target gas is crucial for deriving the correct photon flux from the ion current signal, a calibrated spinning rotor vacuum gauge for monitoring gas pressures in the range of 10^{-4} mbar and a calibrated Pt100 resistance thermometer are installed in the device. In (1), the target gas density n_a is derived from the pressure p and the temperature T (p and T usually remain constant during one experimental session), the photoionization cross section σ_{pi} is tabulated in [29].

The GMD was calibrated in ion current mode at the PTB Laboratories in the VUV spectral range using dispersed synchrotron radiation at low intensity in conjunction with a cryogenic radiometer which is a primary detector standard [24]. The relative standard uncertainty of the calibration factor amounts to 3.4%. Taking into account the uncertainty of the ion current measurement of 1.5%, the pressure measurement of 1.4%, the temperature measurement of 1.0% as well as the uncertainty of the cross section data of 3%, the final relative standard uncertainty for the average photon flux determination with the GMD amounts to 5%. This value is also justified by validation measurements performed recently at the Spring-8 FEL facility in Japan [30, 31].

3. Purity and Single Ionization of the Target Gas

We checked the time-of-flight spectra available from the multiplier signal of the GMD to rule out the influence of contaminating impurities in the target gas and the influence of multiple ionization of the target gas. Both effects would perturb the ion-current signal by adding currents from other ions than singly ionized target gas particles and therefore the absolute calibration would no longer be valid. Figure 2a shows an ion time-of-flight spectrum where the Xe target gas was contaminated with traces of residual air. Besides the Xe ion peak, N_2 and O_2 ion peaks are clearly discernible. The time-of-flight spectrum in 2b was taken with pure Xe as target gas and accordingly only one peak from singly ionized Xe is discernible. Multiply ionized Xe would show up as peaks at shorter times of

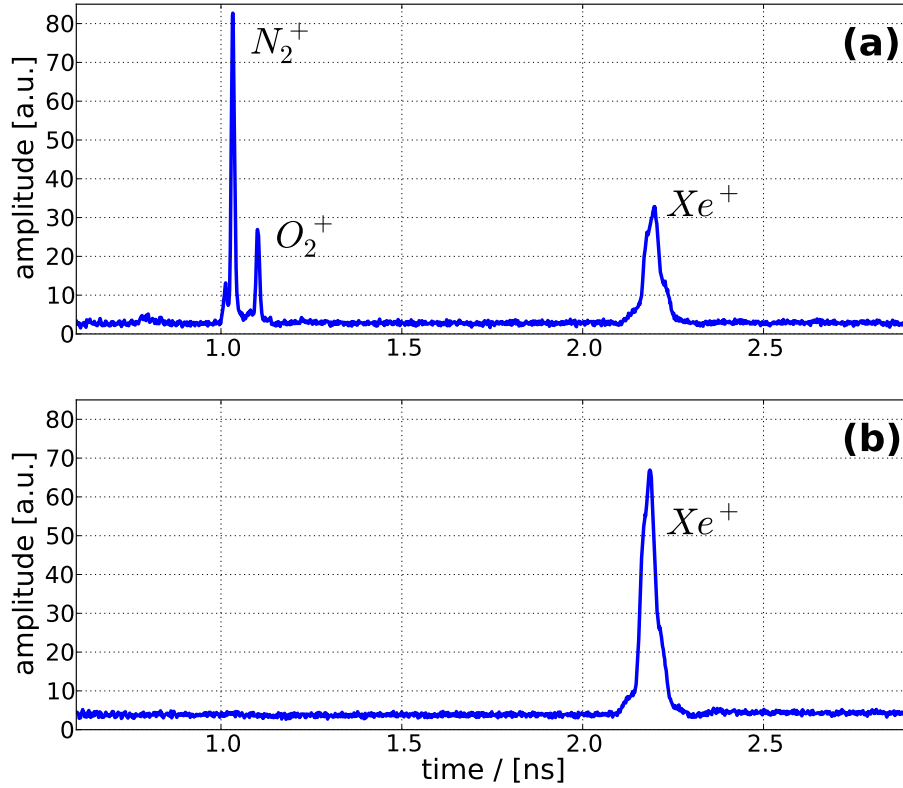


Figure 2. Two exemplary ion TOF spectra (averaged over ~ 5000 shots) from the GMD illustrating the purity of the target gas. The spectrum of Xe target gas and residual air is shown in the (a) while (b) shows the spectrum of Xe target gas as used for the flux measurements.

flight ($TOF \propto (q/m)^{-2}$) and indicate that either the peak irradiance and/or the target gas density inside the detection chamber are too high. Apparently these peaks are not present. The same purity check was performed when Ar was used as target gas in the GMD. This purity of the spectra proves that the values for the photon numbers calculated from the GMD in our experiment are reliable.

4. Shot-to-shot Distribution

Another feature of the detector is the possibility to derive single shot intensities from the multiplier signal. Knowing the averaged photon number N_{AV} , single shot photon numbers, determined from the peak value of the multiplier signal I_{SS} , read as:

$$N_{SS} = N_{AV} \times \frac{I_{SS}}{I_{AV}} . \quad (2)$$

Figure 3 shows the shot-to-shot flux variation from our Laser system measured with a standard IR photodiode (leakage through a mirror) and the corresponding

flux variation of our HHG source measured with the single shot multiplier signal I_{SS} coupled to a digital oscilloscope. The Laser varied by $\pm 2.3\%$ at FWHM, whereas the HHG signal varied by $\pm 26.6\%$. The fact that the VUV signal fluctuates by an order of magnitude more than the generating Laser clearly points out the highly non-linear nature of the HHG process. Note that the source was not optimized for minimal shot-to-shot fluctuations.

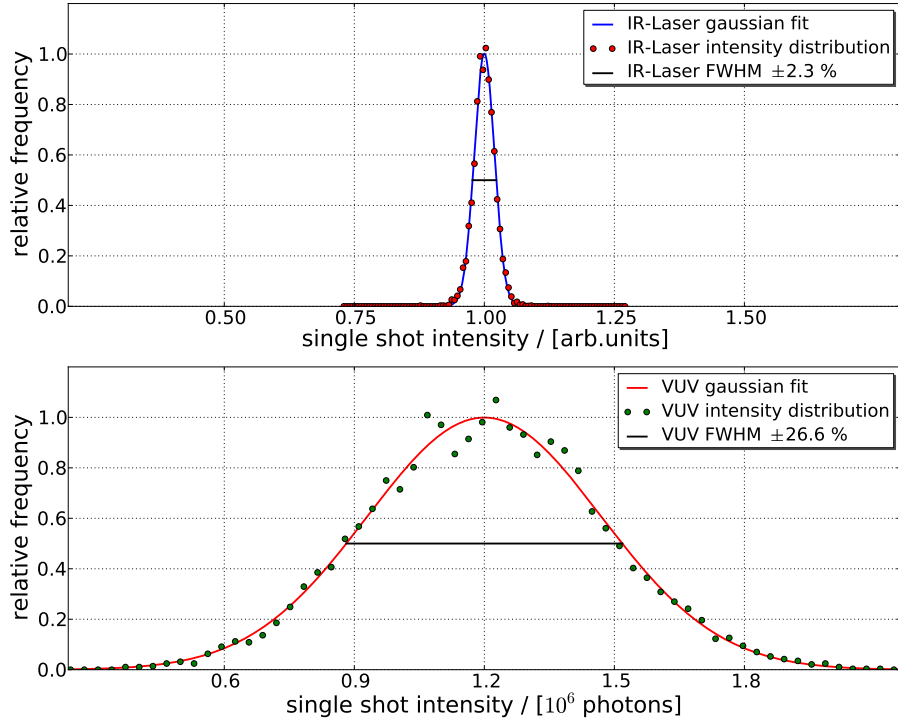


Figure 3. Intensity distribution showing the relative shot-to-shot energy variations of the fundamental IR laser (top) and the VUV radiation produced in the highly non-linear HHG process (bottom). The IR laser intensity distribution in the upper panel is normalized to its maximum and shown in arbitrary units, whereas absolute photon numbers are given for the VUV intensity distribution.

5. Comparison: Diode vs. GMD

Figure 4 and Figure 5 depict the comparison of the average flux measured with the GMD and the GaAsP photodiode. The diode was calibrated in the range from 6 eV to 27 eV by PTB within 1 week after the experiments at the HHG source to foreclose errors due to a diode specific history like, for example, aging processes. The source used for calibration delivered approximately 10 photons/pulse with a pulse duration of 20 ps FWHM and a bandwidth of 0.4 eV at a repetition rate

of 500 MHz . This corresponds to an average flux of 5×10^9 photons/s or an average power of 20 nW at 23.7 eV. The peak flux of one single pulse is thus of the order of 5×10^{11} photons/s corresponding to a peak power of 2 μ W. In contrast, our HHG setup yields monochromatized pulses with 10^6 photons/pulse of 120 fs FWHM duration and a bandwidth of 140 meV at a repetition rate of 3 kHz . This corresponds to an average flux of 3×10^9 photons/s or an average power of 12 nW. Due to the short duration of the pulses, the peak flux of one single pulse is of the order of 10^{19} photons/s, which corresponds to a peak power of 45 W for a photon energy of 23.7 eV as used here. We want to point out, that for both cases, the irradiated area of the diode was 2-3 mm².

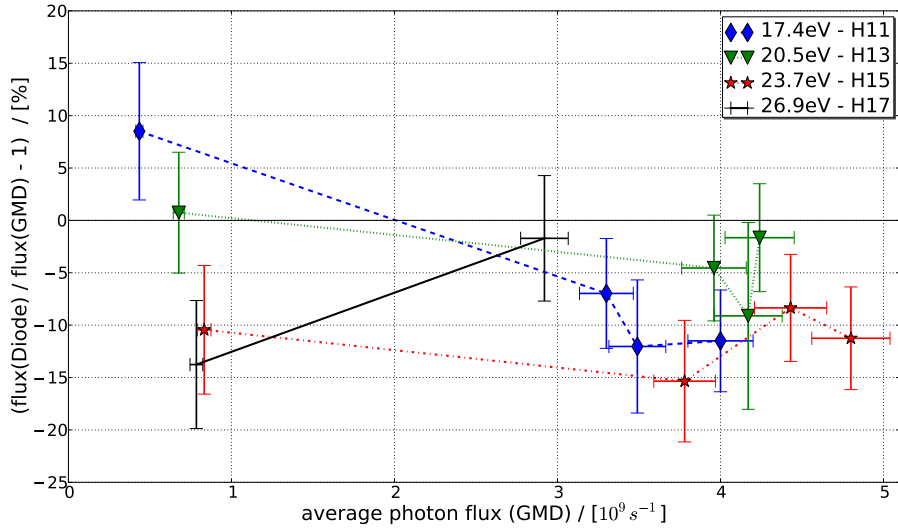


Figure 4. Plot of the relative deviation of the average photon flux determined with the photodiode from the absolute flux given by the calibrated gas detector signal versus the photon flux for different photon energies. The measurements with different laser harmonics are connected with lines and correspond to various flux levels. \blacklozenge : H11, $+$: H13, \star : H15, \blacktriangledown : H17

For comparing both detectors we calculated the relative deviation of the fluxes determined from the diode and the GMD:

$$\Delta = \frac{flux(Diode)}{flux(GMD)} - 1 \quad . \quad (3)$$

In Figure 4 the relative deviation (in percent) between the average photon flux derived from the diode signal and that from the GMD is plotted against the absolute average flux measured with the GMD. Four data sets (connected with lines) are shown for four different photon energies corresponding to different harmonics of our source. To vary the harmonic yield and therefore the fluxes, the width of an aperture in the generating laser beam was tuned. In a next step we calculated the resulting power (product of photon energy and flux) of the VUV radiation. Figure 5 depicts the deviation (in percent) between the average

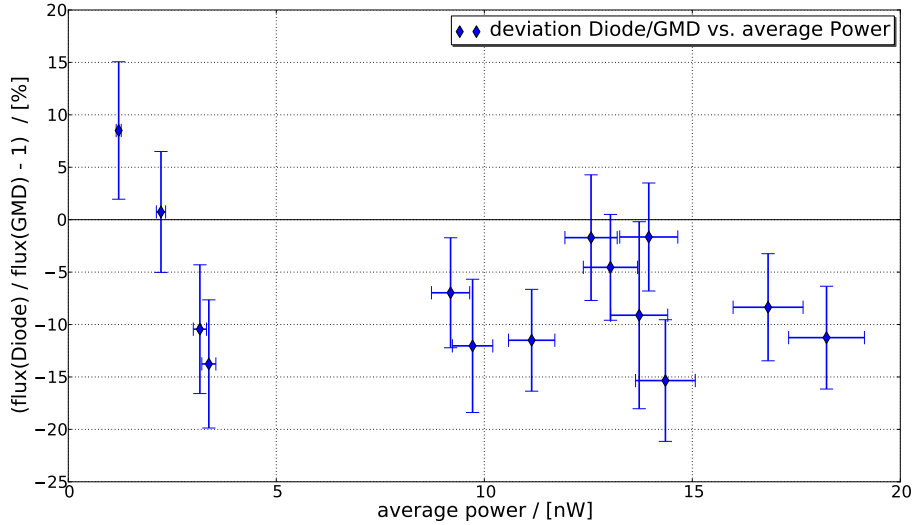


Figure 5. Plot of the relative deviation of the average photon flux measured with the photodiode from the absolute flux given by the calibrated GMD signal versus the average power deposited in the diode for the measurements from Figure 4. The diode systematically underestimates the photon flux by upto -15% for all but the two smallest amounts of power tested in this experiment.

photon flux calculated from the response of the diode and that of the GMD versus the absolute average power given by the GMD signal. The error bars in both graphs are deduced by taking into account the 5% accuracy of the GMD and the accuracy of the measurement of the photo current from the diode. The photo current was measured with a Keithley 6485 electrometer in slow averaging mode. The accuracy of the photo current values were approximated for every measurement by carefully observing the variation of the photo current signal and amounted to be in the range of 3% to 10%. The graphs show, that the diode systematically underrated the photon flux by up to -15% . This points to saturation effects in the diode due to the high peak power emitted from our HHG source.

From work using pulsed classical laser sources [25, 26, 27], it is known that due to an increasing probability of charge carrier recombination in the diode for increasing peak power the charge yield from the diode is lower than expected from the calibration with radiation at comparable average powers. Illuminating a diode with quasi cw light provokes an almost constant creation of charge carriers in the semiconductor material and yields in an equilibrium between charge carriers created by the radiation, recombination of charge carriers and charge arriving at the read-out electronics of the diode. When the diode instead is illuminated with short femtosecond pulses of high peak power separated by relatively long dark periods without illumination, there is more time for the charge carriers to recombine before being read out. The rate of recombination directly depends on

the charge carrier density, which in turn directly depends on the instantaneous power hitting the diode. Thus, for high peak powers, higher recombination rates and therefore saturation losses occur. This explains the saturation effects observed here: the response of the semiconductor diode is lower for short pulses than expected from calibration with longer pulses. Typical saturation behavior like increasing deviation for increasing fluxes could not be determined from our data due to the small dynamic range which was available in this work.

However, our results prove, that a calibrated photodiode is still a good and easy-to-use tool for measuring the flux of femtosecond VUV HHG photon sources within, as in our case, an accuracy of 15%.

6. Summary

For the first time, a gas monitor detector (GMD) was used to measure the absolute photon flux and the absolute power of a femtosecond VUV HHG source with an accuracy of 5%. The GMD allows for the determination of absolute average fluxes, as well as shot-to-shot variations, therefore we were able to estimate the shot-to-shot stability of our 3 kHz repetition rate HHG source.

We compared average photon fluxes of four different photon energies and the corresponding radiant powers of our source derived from a PTB-calibrated Hamamatsu g112704 GaAsP photodiode with the values obtained from the gas monitor detector. In our experiment the photodiode systematically underestimated the real photon flux by up to -15% . This points to saturation losses in the diode due to increased recombination of the charge carriers generated by the incident light, but also shows that such a semiconductor photodiode is still a good tool to estimate the average flux from femtosecond VUV sources with an accuracy of 15% in our case.

Photodiodes have been used for measuring the photon flux in many experiments, the present work clarifies the reliability and accuracy of the photon fluxes determined in these experiments and justifies the use of semiconductor photodiodes for measuring the photon flux of a femtosecond HHG source for future experiments.

References

- [1] L’Huillier A and Balcou Ph. High-order harmonic generation in rare gases with a 1 ps 1053 nm laser. *Phys. Rev. Lett.*, 70(6):774–777, Feb 1993.
- [2] Chen M-C, Arpin P, Popmintchev T, Gerrity M, Zhang B, Seaberg M, Popmintchev D, Murnane M, and Kapteyn H. Bright, coherent, ultrafast soft x-ray harmonics spanning the water window from a tabletop light source. *Phys. Rev. Lett.*, 105(17):173901, Oct 2010.
- [3] Brabec T and Krausz F. Intense few-cycle laser fields: Frontiers of nonlinear optics. *Rev. Mod. Phys.*, 72(2):545–591, Apr 2000.
- [4] Krausz F and Ivanov M. Attosecond physics. *Rev. Mod. Phys.*, 81(1):163–234, Feb 2009.
- [5] Wernet Ph, Odelius M, Godehusen K, Gaudin J, Schwarzkopf O, and Eberhardt W. Real-time evolution of the valence electronic structure in a dissociating molecule. *Phys. Rev. Lett.*, 103(1):013001, Jun 2009.
- [6] Wörner H, Bertrand J, Corkum P, and Villeneuve D. High-harmonic homodyne detection of the ultrafast dissociation of br2 molecules. *Phys. Rev. Lett.*, 105(10):103002, Sep 2010.
- [7] Loh Z-H and Leone S. Ultrafast strong-field dissociative ionization dynamics of CH₂Br₂ probed by femtosecond soft x-ray transient absorption spectroscopy. *J. Chem. Phys.*, 128(20), MAY 28 2008.
- [8] Gagnon E, Ranitovic P, Tong X-M, Cocke C, Murnane M, Kapteyn H, and Sandhu A. Soft X-ray-Driven Femtosecond Molecular Dynamics. *Science*, 317(5843):1374–1378, 2007.
- [9] Miaja-Avila L, Saathoff G, Mathias S, Yin J, La-O-Vorakiat C, Bauer M, Aeschlimann M, Murnane M, and Kapteyn H. Direct measurement of core-level relaxation dynamics on a surface-adsorbate system. *Phys. Rev. Lett.*, 101(4):046101, Jul 2008.
- [10] La-O-Vorakiat C, Siemens M, Murnane M, Kapteyn H, Mathias S, Aeschlimann M, Grychtol P, Adam R, Schneider C, Shaw J, Nembach H, and Silva T. Ultrafast demagnetization dynamics at the *m* edges of magnetic elements observed using a tabletop high-harmonic soft x-ray source. *Phys. Rev. Lett.*, 103(25):257402, Dec 2009.
- [11] Ravasio A, Gauthier D, Maia F, Billon M, Caumes J-P, Garzella D, Géléoc M, Gobert O, Hergott J-F, Pena A-M, Perez H, Carré B, Bourhis E, Gierak J, Madouri A, Mailly D, Schiedt B, Fajardo M, Gautier J, Zeitoun P, Bucksbaum P, Hajdu J, and Merdji H. Single-shot diffractive imaging with a table-top femtosecond soft x-ray laser-harmonics source. *Phys. Rev. Lett.*, 103(2):028104, Jul 2009.
- [12] Sukiasyan S, Patchkovskii S, Smirnova O, Brabec T, and Ivanov M. Exchange and polarization effect in high-order harmonic imaging of molecular structures. *Phys. Rev. A*, 82(4):043414, Oct 2010.
- [13] Itatani J, Levesque J, Zeidler D, Niikura H, Pepin H, Kieffer J, Corkum P, and Villeneuve D. Tomographic imaging of molecular orbitals. *Nature*, 432(7019):867–871, Dec 2004.
- [14] Li W, Zhou X, Lock R, Patchkovskii S, Stolow A, Kapteyn H, and Murnane M. Time-Resolved Dynamics in N₂O₄ Probed Using High Harmonic Generation. *Science*, 322(5905):1207–1211, 2008.
- [15] He X, Miranda M, Schwenke J, Guilbaud O, Ruchon T, Heyl C, Georgadiou E, Rakowski R, Persson A, Gaarde M B, and L’Huillier A. Spatial and spectral properties of the high-order harmonic emission in argon for seeding applications. *Phys. Rev. A*, 79(6):063829, Jun 2009.
- [16] Lambert G, Hara T, Garzella D, Tanikawa T, Labat M, Carre B, Kitamura H, Shintake T, Bougeard M, Inoue S, Tanaka Y, Salieres P, Merdji H, Chubar O, Gobert O, Tahara K, and Couprie M-E. Injection of harmonics generated in gas in a free-electron laser providing intense and coherent extreme-ultraviolet light. *Nature Physics*, 4:296–300, Apr 2008.
- [17] Nabekawa Y, Hasegawa H, Takahashi E J, and Midorikawa K. Production of doubly

- charged helium ions by two-photon absorption of an intense sub-10-fs soft x-ray pulse at 42 eV photon energy. *Phys. Rev. Lett.*, 94(4):043001, Jan 2005.
- [18] Hasegawa H, Takahashi E J, Nabekawa Y, Ishikawa K L, and Midorikawa K. Multiphoton ionization of *he* by using intense high-order harmonics in the soft-x-ray region. *Phys. Rev. A*, 71(2):023407, Feb 2005.
- [19] Nisoli M, Sansone G, Stagira S, De Silvestri S, Vozzi C, Pascolini M, Poletto L, Villoresi P, and Tondello G. Effects of carrier-envelope phase differences of few-optical-cycle light pulses in single-shot high-order-harmonic spectra. *Phys. Rev. Lett.*, 91(21):213905, Nov 2003.
- [20] Riedel D, Hernandez-Pozos J, Palmer R, Baggott S, Kolasinski K, and Foord J. Tunable pulsed vacuum ultraviolet light source for surface science and materials spectroscopy based on high order harmonic generation. *Review of Scientific Instruments*, 72(4):1977–1983, 2001.
- [21] Sommerer G, Mevel E, Hollandt J, Schulze D, Nickles P V, Ulm G, and Sandner W. Absolute photon number measurement of high-order harmonics in the extreme uv. *Optics Communications*, 146(1-6):347 – 355, 1998.
- [22] Schrüfer M, Cheng Z, Hentschel M, Tempea G, Kálmán P, Brabec T, and Krausz F. Absorption-limited generation of coherent ultrashort soft-x-ray pulses. *Phys. Rev. Lett.*, 83(4):722–725, Jul 1999.
- [23] Hergott J-F, Kovacev M, Merdji H, Hubert C, Mairesse Y, Jean E, Breger P, Agostini P, Carré B, and Salières P. Extreme-ultraviolet high-order harmonic pulses in the microjoule range. *Phys. Rev. A*, 66(2):021801, Aug 2002.
- [24] Gottwald A, Kroth U, Richter M, Schoeppe H, and Ulm G. Ultraviolet and vacuum-ultraviolet detector-based radiometry at the metrology light source. *Measurement Science and Technology*, 21(12):125101, 2010.
- [25] Richter M, Kroth U, Gottwald A, Gerth Ch, Tiedtke K, Saito T, Tassy I, and Vogler K. Metrology of pulsed radiation for 157-nm lithography. *Appl. Opt.*, 41(34):7167–7172, Dec 2002.
- [26] Vest R and Grantham S. Response of a silicon photodiode to pulsed radiation. *Appl. Opt.*, 42(25):5054–5063, Sep 2003.
- [27] Vest R, Hill S, and Grantham S. Saturation effects in solid-state photodiodes and impact on euvl pulse energy measurements. *Metrologia*, 43(2):S84, 2006.
- [28] Richter M, Gottwald A, Kroth U, Sorokin A, Bobashev S, Shmaenok L, Feldhaus J, Gerth Ch, Steeg B, Tiedtke K, and Treusch R. Measurement of gigawatt radiation pulses from a vacuum and extreme ultraviolet free-electron laser. *Applied Physics Letters*, 83(14):2970–2972, 2003.
- [29] Tiedtke K, Feldhaus J, Hahn U, Jastrow U, Nunez T, Tschentscher T, Bobashev S, Sorokin A, Hastings J, Moller S, Cibik L, Gottwald A, Hoehl A, Kroth U, Krumrey M, Schoeppe H, Ulm G, and Richter M. Gas detectors for x-ray lasers. *Journal of Applied Physics*, 103(9):094511, 2008.
- [30] Saito N, Juranić P, Kato M, Richter M, Sorokin A, Tiedtke K, Jastrow U, Kroth U, Schoeppe H, Nagasono M, Yabashi M, Tono K, Togashi T, Kimura H, Ohashi H, and Ishikawa T. Radiometric comparison for measuring the absolute radiant power of a free-electron laser in the extreme ultraviolet. *Metrologia*, 47(1):21, 2010.
- [31] Kato M, Saito N, Tiedtke K, Juranić P, Sorokin A, Richter M, Morishita Y, Tanaka T, Jastrow U, Udo Kroth U, Schoeppe H, Nagasono M, Yabashi M, Tono K, Togashi T, Kimura H, Ohashi H, and Ishikawa T. Measurement of the single-shot pulse energy of a free electron laser using a cryogenic radiometer. *Metrologia*, 47(5):518, 2010.
- [32] Wernet Ph, Gaudin J, Godehusen K, Schwarzkopf O, and Eberhardt W. Femtosecond time-resolved photoelectron spectroscopy with a vacuum-ultraviolet photon source based on laser high-order harmonic generation. *Review of Scientific Instruments*, 2011. Submitted to *RSI*.

- [33] Wernet Ph, Godehusen K, Schwarzkopf O, and Eberhardt W. Femtosecond vuv photon pulses for time-resolved photoelectron spectroscopy. In Paul Corkum, David M. Jonas, R. J. Dwayne. Miller, and Andrew M. Weiner, editors, *Ultrafast Phenomena XV*, volume 88 of *Springer Series in Chemical Physics*, pages 45–47. Springer Berlin Heidelberg, 2007. 10.1007/978-3-540-68781-8_15.
- [34] Glover T E, Schoenlein R W, Chin A H, and Shank C V. Observation of laser assisted photoelectric effect and femtosecond high order harmonic radiation. *Phys. Rev. Lett.*, 76(14):2468–2471, Apr 1996.
- [35] Henke B, Gullikson E, and Davis J. X-Ray Interactions: Photoabsorption, Scattering, Transmission, and Reflection at $E = 50\text{-}30,000$ eV, $Z = 1\text{-}92$. *Atomic Data and Nuclear Data Tables*, 54(2):181–342, July 1993.